



HHS Public Access

Author manuscript

J Biol Inorg Chem. Author manuscript; available in PMC 2016 November 21.

Published in final edited form as:

J Biol Inorg Chem. 2008 November ; 13(8): 1291–1299. doi:10.1007/s00775-008-0415-2.

Metal complexation chemistry used for phosphate and nucleotide determination: an investigation of the Yb³⁺–pyrocatechol violet sensor

Ernestas Gaidamauskas,

Department of Chemistry, Colorado State University, Fort Collins, CO 80523-1872, USA

Kanokkarn Saejueng,

Department of Chemistry, USC, Los Angeles, CA 90089-0744, USA

Alvin A. Holder,

Department of Chemistry, Colorado State University, Fort Collins, CO 80523-1872, USA

Subalita Bharuah,

Department of Chemistry, Colorado State University, Fort Collins, CO 80523-1872, USA

Boris A. Kashemirov,

Department of Chemistry, USC, Los Angeles, CA 90089-0744, USA

Debbie C. Crans, and

Department of Chemistry, Colorado State University, Fort Collins, CO 80523-1872, USA

Charles E. McKenna

Department of Chemistry, USC, Los Angeles, CA 90089-0744, USA

Debbie C. Crans: crans@lamar.colostate.edu; Charles E. McKenna: mckenna@usc.edu

Abstract

Metal complexation reactions can be used effectively as sensors to measure concentrations of phosphate and phosphate analogs. Recently, a method was described for the detection of phosphate or ATP in aqueous solution based on the displacement by these ligands of pyrocatechol violet (PV) from a putative 2:1 (Yb³⁺)₂PV complex. We have not been able to reproduce this stoichiometry and report this work in order to correct the coordination chemistry upon which sensor applications are based. In our work, colorimetric and spectrophotometric detection of phosphate was confirmed qualitatively (blue PV + Yb³⁺; yellow + P_i); however, the sequence of visual changes on the titration of PV with 2 equiv. of Yb³⁺ and back titration with ATP as described previously could not be reproduced. In contrast to the linear response to P_i that was reported previously, the absorbance response at 443 or 623 nm was found to be sigmoidal using the recommended 2:1 Yb³⁺:PV solution (100 μM:50 μM, pH 7, HEPES). Furthermore, both continuous variation titration and molar ratio analysis (Job plot) experiments are consistent with

Correspondence to: Debbie C. Crans, crans@lamar.colostate.edu; Charles E. McKenna, mckenna@usc.edu.

Electronic supplementary material

The online version of this article (doi:<http://dx.doi.org/10.1007/s00775-008-0415-2>) contains supplementary material, which is available to authorized users.

1:1, not 2:1, YbPV complex stoichiometry at pH 7 in HEPES buffer, indicating that the deviation from linearity is produced by excess Yb^{3+} . Indeed, using a 1:1 Yb^{3+} :PV ratio produces a linear response in Abs at 443 or 623 nm on back titration with analyte (phosphate or ATP). In addition, speciation analysis of the Yb–ATP system demonstrates that a 1:1 complex containing Yb^{3+} and ATP predominates in solution at μM metal ion and ATP concentrations. Paramagnetic ^1H NMR spectroscopy directly establishes the formation of Yb^{3+} –solute complexes in dilute aqueous solution. The 1:1 YbPV complex can be used for the colorimetric measurement of phosphate and ATP concentrations from $\sim 2 \mu\text{M}$.

Keywords

Phosphate sensing; ATP sensing; Ytterbium; Pyrocatechol violet; Coordination chemistry

Introduction

Phosphates and nucleotides are key metabolites in biology and play a central role in biology and medicine [1, 2]. Since phosphates per se contain no inherent near-UV–vis chromophore, they present a challenge to the development of sensitive and practical methods for detection. Approaches to this problem have included electrochemical [3], conductive [4], refractive index [5–7] and fluorescence [8, 9] detection, but have been limited by poor sensitivity and selectivity. Methods based on chemical derivatization may complicate the analytical procedure [9–11], but when combined with indirect detection they offer the most promising strategy for the development of sensitive and specific analytical methods for this class of compounds [4, 12–15]. Importantly, the strong chelating properties of phosphates, including nucleotides, for particular metal ions can be exploited in detection assays. Various approaches for detecting phosphates and derivatives utilizing selective coordination chemistry have been described [16–22].

Recently, Yin et al. [23–25] reported the indirect detection of HPO_4^{2-} and ATP using an ytterbium (Yb^{3+})–pyrocatechol violet (PV) complex (see Fig. 1 for the structure of PV). These works reported the formation of a blue putative Yb_2PV complex in neutral aqueous solution, which, in the presence of added HPO_4^{2-} and ATP, undergoes ligand exchange [23–25], releasing the free PV dye (which is yellow). The exchange reaction was conveniently monitored by UV–visible spectroscopy, observing the disappearance of the Yb^{3+} –PV complex (623 nm) or the release of the free PV at 423 nm [23].

The chelating properties of phosphates and nucleotides can lead to the formation of more than one kind of metal complex in solution depending on the pH and other specific conditions [26–30]. Specifically, Yb^{3+} has been reported to form several complexes with phosphate and ATP [28]. Given the limitations on the solubility of the Yb^{3+} – P_i system, which impedes analysis by potentiometry, less information is available on this system. However, the Yb^{3+} and ATP system has received more attention [26, 28, 30–32] in studies ranging from spectrophotometric analysis at μM concentrations [30] to studies at much higher concentrations using alternative techniques such as potentiometry [28], electron spin echo [31] and NMR spectroscopy [32]. Not surprisingly, Yb^{3+} complexes with ATP display

both 1:1 and 1:2 stoichiometries. The 1:1 complexes are generally the major complexes at low (μM) concentrations and at high metal-to-ligand ratios (excess metal ion) [26, 30]. The 1:2 complexes predominate at higher concentrations (mM) and at low metal to ligand ratios (excess ligand) [27, 28]. At intermediate concentrations, both 1:1 and 1:2 complexes are observed [28]. Some X-ray structures have been reported for the $\text{Yb}^{3+}\text{-P}_i$ system [33–36]. For example, one report describes a 1:1 complex with metal coordinated to eight O atoms forming two orthogonal interpenetrating tetrahedral geometries [34]. However, the relevance of this structure to the complex in solution is uncertain. There are no structures in the crystal database for $\text{Yb}^{3+}\text{-ATP}$ complexes.

We were originally interested in exploring the applicability of the $\text{Yb}^{3+}\text{-PV}$ sensor to the detection of phosphorus-containing compounds. However, we were unable to quantitatively reproduce the original observations of Yin et al. with phosphate or ATP, prompting us to reinvestigate the underlying complexation chemistry. Here we report on findings indicating that their assumed $\text{Yb}^{3+}\text{-PV}$ complex stoichiometry, which is fundamental to the accurate application of this system to phosphate and ATP determination, is incorrect.

Materials and methods

Solid pyrocatechol violet (Sigma–Aldrich, St. Louis, MO, USA, and Alfa Aesar, Karlsruhe, Germany), ytterbium(III) chloride hexahydrate (99.998%, Sigma–Aldrich), and ytterbium(III) oxide (99.998%, REacton[®], Alfa Aesar) were used to prepare the 10 mM stock solutions. The UV–vis spectra were acquired at ambient temperature on a PerkinElmer (Waltham, MA, USA) Lambda 25 spectrophotometer employed in a dual beam mode using 10 mM HEPES buffer as a blank. Water purified with the E-pure system from Barnstead (Dubuque, IA, USA; up to $17.8\text{ M}\Omega\text{ cm}^{-1}$) was used throughout. The NMR studies were carried out using paramagnetic parameters, as reported previously [37]. Specifically, the ^1H NMR studies were carried out using a short acquisition time (0.05 s) and large sweep widths. The ^{31}P NMR studies were carried out using an acquisition time of 0.1 s.

Stock solutions

PV was dissolved in deionized water. The resulting solution was transferred to the volumetric flask and diluted with water. The PV stock solution was standardized at pH 5.3 in 10 mM acetate buffer solution, based on a molar absorbance value of $14,000\text{ M}^{-1}\text{ cm}^{-1}$ at 445 nm [38]. Concentrations calculated based on weight were within 3–5% of those obtained by molar absorbance. The stock solution was prepared fresh before each analysis. This solution was found to be stable for several days.

The Yb^{3+} stock solution was prepared from either $\text{YbCl}_3\cdot 6\text{H}_2\text{O}$ or Yb_2O_3 with identical results. $\text{YbCl}_3\cdot 6\text{H}_2\text{O}$ was dissolved in deionized water, while Yb_2O_3 was dissolved in conc. HCl with stirring and under heating, and slowly evaporated until a neutral vapor reaction was obtained. The resulting solution was transferred to the volumetric flask and diluted with water. The Yb^{3+} stock solution was standardized by EDTA titration at pH 6.0 in acetate buffer using xylenol orange as a complexometric indicator [39]. Similar results were obtained using PV as a complexometric indicator. The Yb^{3+} solution was stable for weeks;

solutions were used for up to two weeks after preparation. Substrate stock solutions (10 mM) were prepared in aqueous solution from the salts.

General procedure for UV–vis spectroscopic analysis sample preparation

Step 1: Blue YbPV complex samples Samples of 50 μM PV and 0–100 μM Yb^{3+} were prepared by adding aliquots of stock solutions of YbCl_3 and PV to 5.0 mL of 10 mM HEPES buffer at pH 7.0. In a typical procedure, the YbCl_3 stock was added to the buffer first, and the PV stock was added after shaking. The resulting solution was shaken for a minimum of 10 s, transferred to the quartz cuvette, and the UV–vis spectrum was recorded immediately.

Step 2: Measuring analyte concentrations Analyte (0–100 μM) was added directly to the freshly prepared YbPV solution. The development of the yellow color from the Yb–analyte complex is complete within 30 s. No significant changes were observed within the 15 min needed to make the measurement.

Results and discussion

Stability and ruggedness of the sensor system

Seeking to explain discrepancies between our results and those reported by Yin et al. for their putative Yb^{3+}_2 –PV phosphate sensor, we first looked for inadvertent errors in the assays as carried out in our laboratory. Assay results obtained using the procedure described in “Materials and methods” are in fact reliably reproducible. After development, the sensor color is stable for at least 2 h, particularly if the PV is kept at a stoichiometry with the metal of 1:1 or less, although a precipitate can be observed after standing overnight. No differences were observed in spectroscopic signature in samples that had been purged and maintained under a blanket of argon. The data presented in Figs. 2, 3 and 4 were obtained in duplicate or triplicate and the error bars in most cases are covered by the plotted symbol. The assay was also carried out by several different operators, and using two different Yb^{3+} salts from two suppliers (“Materials and methods”) with identical results. Deviations from the procedures as described can introduce variability into the results, in particular during the preparation of the stock solution in HEPES buffer (pH 7.0), since both PV and Yb^{3+} solutions can change irreversibly over time. At pH 7, the PV solution changes color from red to yellow and finally to brown, indicating oxidation. Oxidation was previously reported to take place above pH 7.5 [40]; however, little or no oxidation was observed at pH 7.0 in HEPES buffer on the timescale of the experiment. The Yb^{3+} solution deposits precipitates of sparingly soluble ytterbium hydroxide after storage for about one week [41].

When stock solutions of PV and YbCl_3 were premixed before adding them to the buffer, the absorbance maximum of the resulting Yb^{3+} –PV complex shifted from 614 to 638 nm. The selection of appropriate solution preparation and mixing times and analyte concentrations of the substrate is critical if the assay is to yield repeatable results. Thus, errors in the assay could be introduced unless consistent time protocols are used.

The procedures described here call for the preparation of solutions which, unless buffer is added to keep the added analyte volume constant, have at the most a 1.5–2% dilution factor.

A 2% dilution is within the experimental error. Since the ratio of Yb^{3+} to PV (YbPV complex) is kept constant in all samples, the only variable is analyte concentration.

A few cautionary notes for the application of this method to the determination of phosphate and phosphorus-containing compounds are needed. First, the complexes that form between Yb^{3+} and phosphorus-containing compounds are very insoluble. If the assay is done at equilibrium conditions, the precipitation of the Yb^{3+} -phosphorus compounds could shift the measurements using this method. This fact is one of the reasons why we recommend that the assay is carried out within a short time period (15 min) with the concentration ranges defined in this work. In our hands, results obtained during 15 min time periods are accurate, whereas measurements made when samples have been left for longer than 1 h may be less reliable. Presumably the kinetics of precipitation are relatively slow, so that this issue is less of a problem in practice.

One can observe interference in phosphorus compound determination when other metal ions are present. Specifically, we found problems with the assay when Zn^{2+} , Cu^{2+} and Ca^{2+} were present at 20, 10 μM , and 10 mM, respectively. Although the total intracellular concentrations of Ca^{2+} (0.1 mM), Zn^{2+} (0.1 mM) and Cu^{2+} (10 μM) [42] imply that Zn^{2+} and Cu^{2+} should, in principle, interfere with assay, this may not actually happen, because the latter two metal ions are known to be strongly chelated in cells [42]. Thus, even when extracts of biological samples are used directly without prior dilution, Zn^{2+} and Cu^{2+} are strongly chelated by metalloproteins and other abundant small-molecule chelators. These complexes are likely to compete favorably with the PV molecule and little metal ion exchange takes place. The presence of Ca^{2+} is not likely to interfere with the assay because the concentration is less than that needed for interference. Overall, we conclude that the metal ion content in these samples is not likely to cause interference when assaying many biological samples.

However, the ability of Yb^{3+} to form coordination complexes with proteins and other biometabolites that naturally chelate Ca^{2+} , Cu^{2+} and Zn^{2+} does limit the application of this assay. If Yb^{3+} displaces Ca^{2+} , Cu^{2+} and Zn^{2+} from the proteins or other intracellular chelators, this Yb^{3+} will no longer interact with PV and will therefore skew the assay measurement. This effect is similar to the well-known transmetallation phenomenon observed for Gd-based MRI contrast agents [43]. Of the three potential problems with this assay, we view the latter to be the most serious, perhaps because this is less easily controlled. We recommend that a standard curve of added P_i should be tested before extensive use on biological samples.

Effect of phosphate and ATP on the Yb^{3+} and PV assembly in HEPES buffer at pH 7.0

The ability of the putative Yb_2PV complex to act as a colorimetric sensor for phosphate was then reinvestigated using the conditions of Yin et al. [23–25]. The absorbances at 443 and 623 nm of a mixture of 100 μM Yb^{3+} and 50 μM PV in 10 mM HEPES, pH 7.0, were monitored as a function of phosphate concentration, resulting in the spectroscopic changes observed in Fig. 2a and in the changes in absorbance shown in Fig. 2b. We also observed a blue to yellow color change consistent with sequestration of Yb^{3+} from the relatively weak Yb–PV complex to form a more stable Yb^{3+} -phosphate complex, with displacement of the

PV dye. However, in surprising contrast to the linear response to phosphate reported previously [23–25], the absorbance difference versus phosphate concentration was found to be sigmoidal (Fig. 2b). The effect of ATP on the Yb₂PV system was also measured, and the data is presented in the Supplementary material (Figs. S1, S2). As shown in Fig. 2b, this analyte also produced a sigmoidal curve rather than the linear response reported previously [23–25].

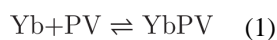
The small initial absorbance change upon the addition of phosphate to 20 μM suggests that free Yb³⁺ exists in this solution, complexing the added phosphate or ATP. When the total phosphate concentration increases from 20 to 120 μM, the UV–vis spectra change significantly, suggesting that free metal ions are increasingly unavailable and that the metal is now being displaced from the Yb–PV complex, resulting in the observed color transition from blue (Yb–PV complex) to yellow (PV). These observations are inconsistent with the results of Yin et al. [23–25] and prompted us to redetermine the Yb and PV complex stoichiometry.

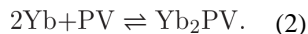
The Yb³⁺ and PV complex stoichiometry is 1:1

We determined the Yb³⁺ and PV complex stoichiometry by both the continuous variation and the molar ratio methods [44]. The continuous variation studies of the Yb³⁺ and PV complex stoichiometry were carried out in 10 mM HEPES solution at pH 7.0. The total concentrations of both Yb³⁺ and PV were kept at 100 μM. In Fig. 3a, we display the absorbance as a function of PV mole fraction at three representative wavelengths. In all cases, the absorbance maximum is located at a mole fraction of 0.5. The 2:1 stoichiometry of a Yb₂PV complex would require the absorbance maximum to occur at 0.33. Therefore, the simplest interpretation of this data is the formation of a 1:1 complex in 10 mM HEPES at pH 7.0.

Although alternative interpretations, including several complexes with stoichiometries that yield an average 1:1 stoichiometry are possible, such as the 2:2 complex, the most likely interpretation for the data presented is a 1:1 complex. The possibility that the complex is a ternary complex of Yb³⁺–PV–P_i is less likely. This conclusion was reached because the spectrophotometric signature of a sample of a 1:1 mixture of Yb³⁺–PV with equimolar P_i is nearly identical to the spectroscopic properties of a solution of uncomplexed PV.

The formation of the 1:1 complex formation was supported by studies using the molar ratio method, where the PV was kept constant and equal to 50 μM, and the Yb³⁺ was varied from 0 to 100 μM in the 10 mM HEPES buffer (pH 7.0). The only complex detected under these conditions was the 1:1 complex, since the transition from the line with the positive slope to the line with zero slope is observed at a 1:1 ratio of Yb³⁺ to PV (Fig. 3b). These results support the equilibrium shown in Eq. 1, but not that shown in Eq. 2, as the determinant process in sensor formation. (It was not possible to extend these studies using speciation titration methods due to the limited solubility of the YbPV.)





To eliminate the possibility that other factors such as adventitious metal ions could explain the discrepancy between our findings and those of Yin et al., we verified that doubly distilled water from a different source, the treatment of HEPES buffer solution with Chelex 100 ion exchange resin, or the use of starting materials from a different supplier did not change the results. We note that our conclusions are supported by some early work on a range of other Yb^{3+} complexes [45–48].

UV–vis absorption of the Yb^{3+} –PV system upon the addition of phosphate and ATP

The question of whether the correct complex has a 1:1 or 2:1 stoichiometry is crucial to the quantitative analysis of phosphates using this system. If the complex formed is actually a 1:1 complex, but a ratio of 2:1 is used in 10 mM HEPES buffer at pH 7.0, then the solution will contain free, uncomplexed Yb^{3+} . As we demonstrate here, added analyte will first coordinate to the free cation and nonlinearity in the titration will result. In Fig. 4a, we show the absorbance spectra observed for solutions containing a 1:1 Yb^{3+} :PV ratio. The absorbance change at two wavelengths as a function of analyte concentration was calculated for both ratios (2:1 and 1:1 Yb :PV) and is shown in Fig. 4b, c. At a 2:1 ratio of Yb^{3+} –PV, a nonlinear response of DA versus concentration is observed, in contrast to the linear plots obtained with the 1:1 ratio. For the 1:1 ratio, a small (10 μM) concentration of added analyte results in a proportional change in absorbance, indicating that the Yb^{3+} ions were initially bound to PV (Fig. 4a, phosphate as the added analyte). When all of the PV has been displaced from the YbPV complex, no further change in absorbance is observed, again consistent with 1:1, not a 2:1, Yb :PV stoichiometry (see Eqs. 3 and 4).



In Fig. 4c, we show the absorption change as a function of ATP concentration at ratios of both 1:1 and 1:2 Yb^{3+} to ATP (Fig. S1). As with P_i (Fig. S2), when the ratio of Yb^{3+} –PV is 2:1, a nonlinear response of A versus concentration is observed, in contrast to the linear plots obtained when the ratio is 1:1. For the 1:1 ratio, even a low concentration of added analyte (10 μM) results in a significant change in absorbance, suggesting that all of the Yb^{3+} ions are pre-bound to the PV, as shown in Fig. 4a, with phosphate as the added analyte. When all of the PV is displaced from the YbPV complex, no further change in absorbance is observed, which is again consistent with a 1:1 stoichiometry.

In the case of the Yb^{3+} –ATP system, several reports of complexes forming in aqueous solutions exist [26, 28, 30]. The higher solubility of Yb^{3+} –ATP complexes has made speciation studies of this system possible, which were carried out in 0.1 KCl [28]. These

studies were carried out from pH 2 to 12 and involved a metal-to-ligand ratio from 1:1 to 1:5. Using formation constants derived from this work, we were able to predict speciation for 1:1 and 1:2 Yb^{3+} :ATP ratios at 50 μM Yb^{3+} (Fig. S3). These speciation diagrams show that at submillimolar concentrations of metal and analyte, the predominant species in solution is mainly the 1:1 complex. However, as the concentration increases to 1 mM, much more of the 1:2 complex forms at 1:1 and 1:2 Yb^{3+} :ATP. At 1 mM Yb^{3+} and 2 mM ATP, almost 80% of the Yb^{3+} exists as a 1:2 complex.

To verify that the conditions illustrated in the speciation diagram are practicable, we prepared equivalent solutions at various pH values and confirmed that indeed such solutions can be prepared without any precipitation over most of the pH range (Fig. S3).

In addition to the speciation constants recommended by Martell and coworkers [49], some previous work had reported hydrolysis constants for a few additional species [50]. These species are minor at pH 7, but their importance increases as the pH increases and the concentration decreases. We chose to use the constants recommended by Martell and coworkers [49], and hesitated to include these species in a study that was carried out without considering these species [28]. However, to evaluate how the presence of such species might impact our studies, we have carried out speciation calculations including these values [50], and these speciation diagrams are shown in Fig. S4. The speciation diagrams in Figures S3 and S4 show little difference at pH 7 at both low and high concentrations. However, at pH 8, the hydrolyzed Yb^{3+} -ATP species is accompanied by soluble Yb^{3+} hydroxides. Thus, at these higher pH values, the Yb^{3+} would not be completely complexed and the assay would no longer be accurately reporting the phosphorus content. This problem is more significant at low concentrations and underlines the importance of maintaining the assay conditions at pH 7.0, as instructed in the “Materials and methods” section.

Potentiometric studies were attempted with the Yb^{3+} - P_i system. Unfortunately, the low solubilities of these complexes preclude proper evaluation of the P_i system in order to compare them with studies reported previously for Yb^{3+} -ATP, where formation constants were obtained from solubility data [51, 52]. However, the available information supports a 1:1 complex, in agreement with the results from our studies (Figs. 2, 4a).

^1H NMR studies of the Yb -PV complex system were attempted (data not shown). Given that Yb is paramagnetic, the presence of this ion effectively increases the relaxation times of all solution components, and line broadening would be anticipated for both free and coordinated PV [37]. The spectra obtained were so dramatically affected by the Yb^{3+} that most of the signals were broadened into the baseline, consistent with the coordination of the metal ion to the PV ligand.

The complexation reaction of Yb^{3+} with ATP was also examined by ^1H and ^{31}P NMR. Complexation of Yb^{3+} by ATP has been detected previously using magnetic methods [32]. Yb^{3+} ion increases the linewidth of signals as a function of its distance from particular nuclei. This effect is apparent in the ^1H NMR spectra presented in Fig. 5. Of the three signals in the 6.5–10 ppm region observed for free ATP in the absence of Yb^{3+} (6.0, 8.1 and 8.4 ppm), the signal at 8.4 ppm broadens immediately into the baseline upon the addition of

even a low ratio (1:10) of Yb^{3+} to ATP. This observation indicates that this aromatic ring proton (H8) is either adjacent to a nitrogen atom that is directly coordinated to the Yb^{3+} , or else it is located near the paramagnetic center. (The former possibility was discounted by Svetlova et al. [28] considering the weak basicity of the purine nitrogen atoms). The other two signals broaden progressively as the ratio reaches 1:1 and are shifted downfield (Fig. 5). The variability in the line broadening of these signals supports the interpretation that the nitrogen atom is not directly coordinated to the Yb^{3+} . At ratios higher than 1:1, the signals continue to broaden but the chemical shifts of the signals show little further change.

Analogous studies were attempted using ^{31}P NMR spectroscopy; however, at the concentrations used to obtain the ^1H NMR spectra, the phosphate signals were excessively broadened (data not shown). Previously, higher concentrations of ATP were reported to exhibit ^{31}P NMR spectra at low metal to ATP ratios [32]. In summary, these NMR studies are consistent with the observation of a 1:1 complex between Yb^{3+} and ATP, in which the Yb^{3+} coordinates directly to the ATP in a multidentate manner involving the triphosphate groups.

Color changes and back titration of the Yb–PV systems with ATP

In light of the corrected sensor stoichiometry required by this work, we also reinvestigated the colorimetric response of the Yb^{3+} –PV system assessed visually using the 2:1 [23–25] and 1:1 stoichiometries. Figure 6a shows the appearance of a series of solutions of PV (50 μM , pH 7, HEPES) containing increasing concentrations of Yb^{3+} (0–50 μM) using a 1:1 ratio of reagents. Back titration of the solution using ATP reverses the original (yellow to blue) color change. Figure 6b shows the corresponding series with $[\text{Yb}^{3+}]$ varied from 0 to 100 μM using the 2:1 ratio of reagents. The color transition from yellow to blue is almost completed at 40 μM Yb^{3+} , and further addition of Yb^{3+} does not appreciably change the color of the solution. Back titration of this solution with ATP manifests a more gradual color transition compared to the equimolar sensor in Fig. 6a.¹ These visual images of the color development in the assay support the idea that the sensor stoichiometry is 1:1 Yb:PV, not 2:1 as claimed previously [23–25].

Conclusion

The stoichiometry of the Yb^{3+} –PV coordination complex is critical for applications of this method to phosphate detection and sensing. The stoichiometry of the complex that forms between Yb^{3+} and PV in aqueous solution at pH 7.0 has been suggested to be either 1:1 [45–48] or 2:1 [23–25]. Our results demonstrate the Yb^{3+} –PV complex stoichiometry to be 1:1. Based on the revised stoichiometry, we reinvestigated the colorimetric response of this sensor to added phosphates and ATP. The stoichiometries of the complexes that Yb^{3+} forms with phosphate and ATP were also investigated using indirect methods. Both of these compounds react with YbPV to form complexes with a predominant 1:1 stoichiometry at μM concentrations of metal and ligand, even though ATP is a multidentate ligand. The utilization of the correct Yb^{3+} :PV stoichiometry is essential to obtain accurate phosphate

¹The photos illustrating the back titration with ATP in Fig. 6 do not compare to those reported previously [23]. It is curious that the details in the figure with the back titration reported previously in Fig. 2 of [23] show imperfections in the cuvettes and sample volumes consistent with an image reversal of samples shown in the initial titration.

derivative concentrations (0–50 μM) based on a linear response of the sensor complex Yb^{3+}PV to the analyte.

Supplementary Material

Refer to Web version on PubMed Central for supplementary material.

Acknowledgments

Debbie C. Crans and Charles E. McKenna thank the National Institutes of Health for funding this work (Grant 1U19CA105010). We also thank Myron Goodman for stimulating discussions and providing the impetus for carrying out this work.

References

1. Blackburn GM, Eckstein F, Kent DE, Perree TD. *Nucleos Nucleot Nucl.* 1985; 4:165–167.
2. Ma QF, Babbitt PC, Kenyon GL. *J Am Chem Soc.* 1988; 110:4060–4061.
3. Usui T, Watanabe T, Higuchi S. *J Chromatogr.* 1992; 584:213–220. [PubMed: 1484106]
4. Tsai EW, Ip DP, Brooks MA. *J Chromatogr.* 1992; 596:217–224. [PubMed: 1400839]
5. Quitasol J, Krastins L. *J Chromatogr.* 1994; 671:273–279.
6. Han MS, Yim DH. *Bull Korean Chem Soc.* 2004; 25:1151–1155.
7. Han MS, Kim DH. *Angew Chem Int Ed Engl.* 2002; 41:3809–3811. [PubMed: 12386855]
8. Lovdahl MJ, Pietrzyk DJ. *J Chromatogr A.* 1999; 850:143–152. [PubMed: 10457475]
9. Peng SX, Dansereau SM. *J Chromatogr A.* 2001; 914:105–110. [PubMed: 11358203]
10. Daley-Yates PT, Gifford LA, Hoggarth CR. *J Chromatogr.* 1989; 490:329–338. [PubMed: 2768406]
11. Qin X-Z, Tsai EW, Sakuma T, Ip DP. *J Chromatogr A.* 1994; 686:205–212.
12. Tsai EW, Chamberlin SD, Forsyth RJ, Bell C, Ip DP, Brooks MA. *J Pharm Biomed Anal.* 1994; 12:983–991. [PubMed: 7819384]
13. Kline WF, Matuszewski BK, Bayne WF. *J Chromatogr.* 1990; 534:139–149. [PubMed: 2094701]
14. Kline WF, Matuszewski BK. *J Chromatogr B.* 1992; 583:183–193.
15. Sparidans RW, den Hartigh J. *Pharm World Sci.* 1999; 21:1–10. [PubMed: 10214661]
16. Palacios MA, Nishiyabu R, Marquez M, Anzenbacher P. *J Am Chem Soc.* 2007; 129:7538–7544. [PubMed: 17530846]
17. Callan JF, de Silva AP, Magri DC. *Tetrahedron.* 2005; 61:8551–8588.
18. Pelleteret D, Fletcher NC, Doherty AP. *Inorg Chem.* 2007; 46:4386–4388. [PubMed: 17474739]
19. Chen ZF, Wang XY, Chen JW, Yang XL, Li YZ, Guo ZJ. *New J Chem.* 2007; 31:357–362.
20. Ambrosi G, Dapporto P, Formica M, Fusi V, Giorgi L, Guerri A, Micheloni M, Paoli P, Pontellini R, Rossi P. *Inorg Chem.* 2006; 45:304–314. [PubMed: 16390069]
21. Ganesh V, Sanz MPC, Mareque-Rivas JC. *Chem Commun.* 2007:5010–5012.
22. O'Neil EJ, Smith BD. *Coord Chem Rev.* 2006; 250:3068–3080.
23. Yin CX, Gao F, Huo FJ, Yang P. *Chem Commun.* 2004:934–935.
24. Yin CX, Huo FJ, Yang P. *Sens Actuators B.* 2005; 109:291–299.
25. Yin CX, Huo FJ, Yang P. *Anal Bioanal Chem.* 2006; 384:774–779. [PubMed: 16365777]
26. Morrison JF, Cleland WW. *Biochemistry.* 1983; 22:5507–5513.
27. Eads CD, Mulqueen P, Dehorrocks W, Villafranca JJ. *J Biol Chem.* 1984; 259:9379–9383. [PubMed: 6746653]
28. Svetlova IE, Smirnova NS, Dobrynina NA, Martynenko LI, Evseev AM. *Russ J Inorg Chem.* 1988; 33:643–645.
29. Smith RM, Martell AE, Chen Y. *Pure Appl Chem.* 1991; 63:1015–1080.
30. Ohyoshi E, Jyodoi K, Kohata S. *Nippon Kagaku Kaishi.* 1993:468–470.

31. Shimizu T, Mims WB, Davis JL, Peisach J. *Biochim Biophys Acta*. 1983; 757:29–39.
32. Tanswell P, Thornton JM, Korda V, Williams RJP. *Eur J Biochem*. 1975; 57:135–145. [PubMed: 240716]
33. Hoppe U, Brow RK, Ilieva D, Jovari P, Hannon AC. *J Non-Cryst Solids*. 2005; 351:3179–3190.
34. Milligan WO, Mullica DF, Beall GW, Boatner LA. *Acta Crystallogr*. 1983; C39:23–24.
35. Rghioui L, El Ammari L, Benarafa L, Wignacourt JP. *Acta Crystallogr*. 2002; C58:i90–i91.
36. Salmon R, Parent C, Vlasse M, Le Flem G. *Mater Res Bull*. 1979; 14:85–89.
37. Crans DC, Yang LQ, Gaidamauskas E, Khan R, An WZ, Simonis U. *ACS Symp Ser*. 2003; 858:304–326.
38. Hulanicki A, Glab S, Ackermann G. *Pure Appl Chem*. 1983; 55:1137–1230.
39. Lyle SJ, Rahman M. *Talanta*. 1963; 10:1177–1182.
40. Ueno, K.; Imamura, T.; Cheng, KL. *Handbook of organic analytical reagents*. Boca Raton: CRC Press; 1992. p. 47-56.
41. Torres J, Brusoni M, Peluffo F, Kremer C, Dominguez S, Mederos A, Kremer E. *Inorg Chim Acta*. 2005; 358:3320–3328.
42. Finney LA, O'Halloran TV. *Science*. 2003; 300:931–936. [PubMed: 12738850]
43. Idee JM, Port M, Raynal I, Schaefer M, Le Greneur S, Corot C. *Fundam Clin Pharmacol*. 2006; 20:563–576. [PubMed: 17109649]
44. Skoog, DA.; West, DM.; Holler, FJ.; Crouch, SR. *Fundamentals of analytical chemistry*. 8th. Belmont: Thomson Brooks/Cole; 2004. p. 805
45. Akhmedli MK, Granovskaya PB. *Azerb Khim Zh*. 1965:105–108.
46. Babko AK, Akhmedli MK, Granovskaya PB. *Ukr Khim Zh*. 1966; 32:879–885.
47. Kirillov AI, Shaulina LP, Churakova GN. *Izv VUZ Khim Kh Tekh*. 1981; 24:1448–1450.
48. Takano T. *Bunseki Kagaku*. 1966; 15:1087–1092.
49. Smith, RM.; Martell, AE. *NIST critically selected stability constants of metal complexes database, version 8.0*. Gaithersburg: NIST; 2004.
50. Baes, CF., Jr; Mesmer, RE. *The hydrolysis of cations*. New York: Wiley; 1976. p. 137
51. Firsching FH, Brune SN. *J Chem Eng Data*. 1991; 36:93–95.
52. Byrne RH, Kim KH. *Geochim Cosmochim Acta*. 1993; 57:519–526.

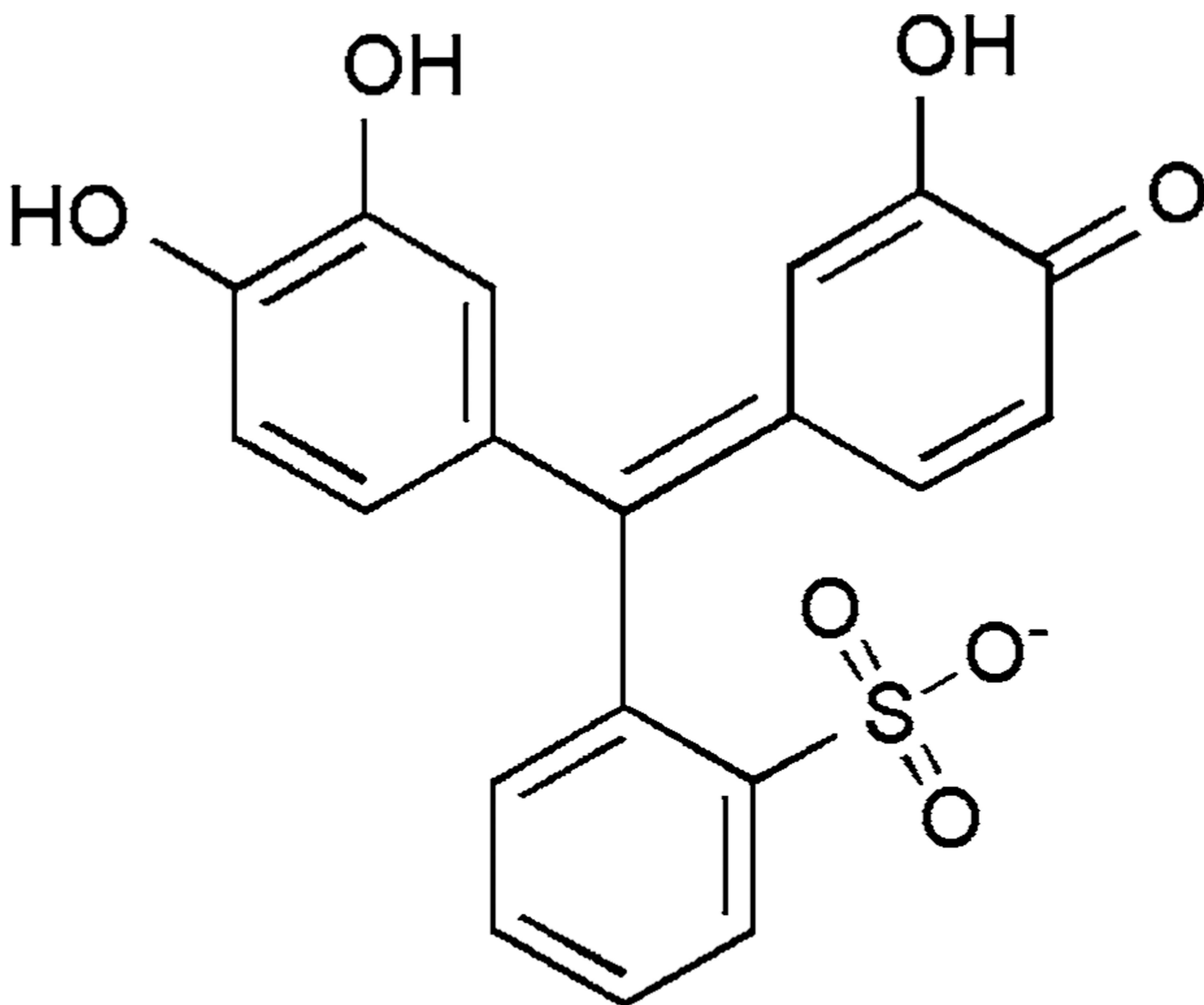


Fig. 1.
Structure of the pyrocatechol violet (PV) monoanion, the predominant species at pH 7.0

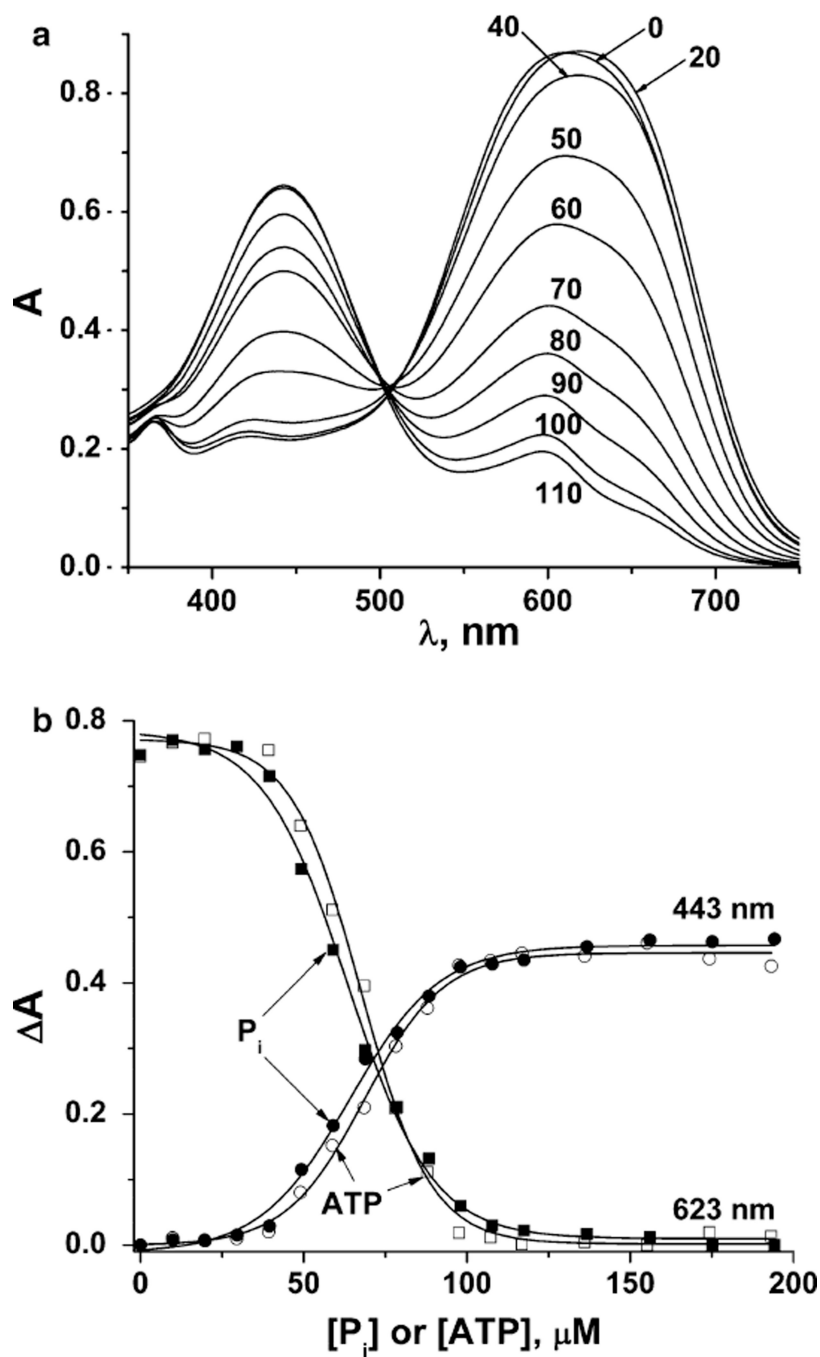


Fig. 2. The absorbances of solutions with a 2:1 Yb^{3+} :PV ratio (100 μM Yb^{3+} and 50 μM PV) in 10 mM HEPES buffer (pH 7.0) (a). The absorbance difference in the 100 μM Yb^{3+} and 50 μM PV solution in 10 mM HEPES buffer (pH 7.0) at two wavelengths (443 and 623 nm) upon phosphate (*full symbols*) and ATP (*open symbols*) addition (b)

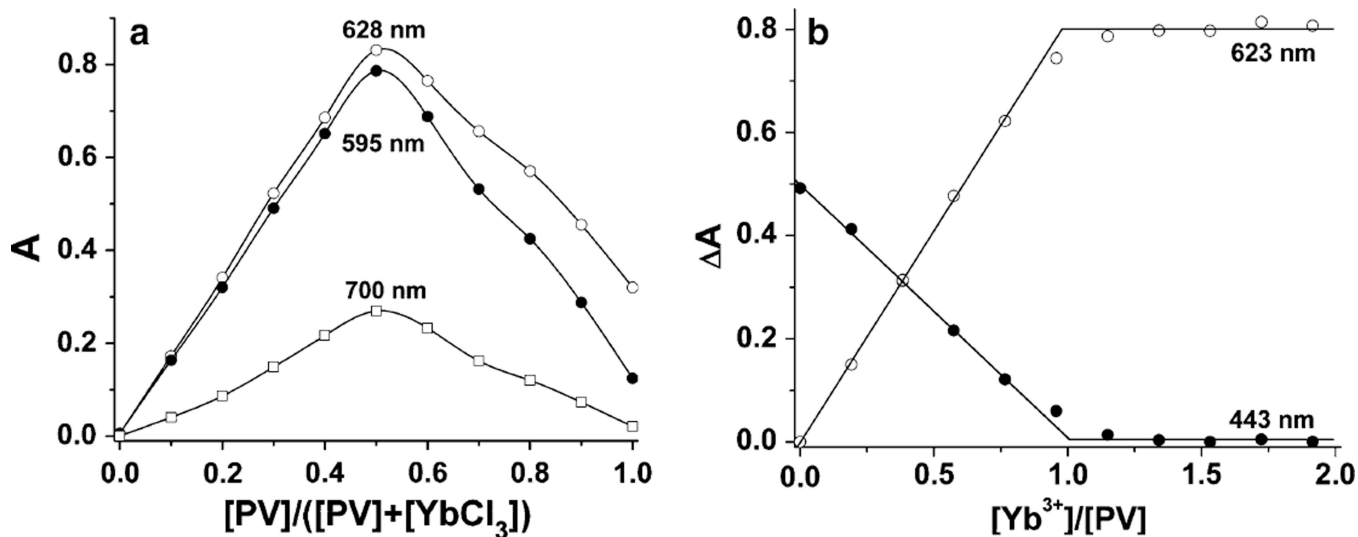


Fig. 3.

a Continuous variation plot at three representative wave-lengths for the Yb^{3+} and PV system in 10 mM HEPES buffer at pH 7.0. The total concentration of Yb^{3+} + PV is equal to 100 μM . Samples were prepared by adding the acidic stock solutions to the buffer. **b** Absorbance difference at 623 and 443 nm as a function of the $[Yb^{3+}]/[PV]$ molar ratio. The PV concentration was kept constant at 50 μM , and Yb^{3+} was varied from 0 to 100 μM

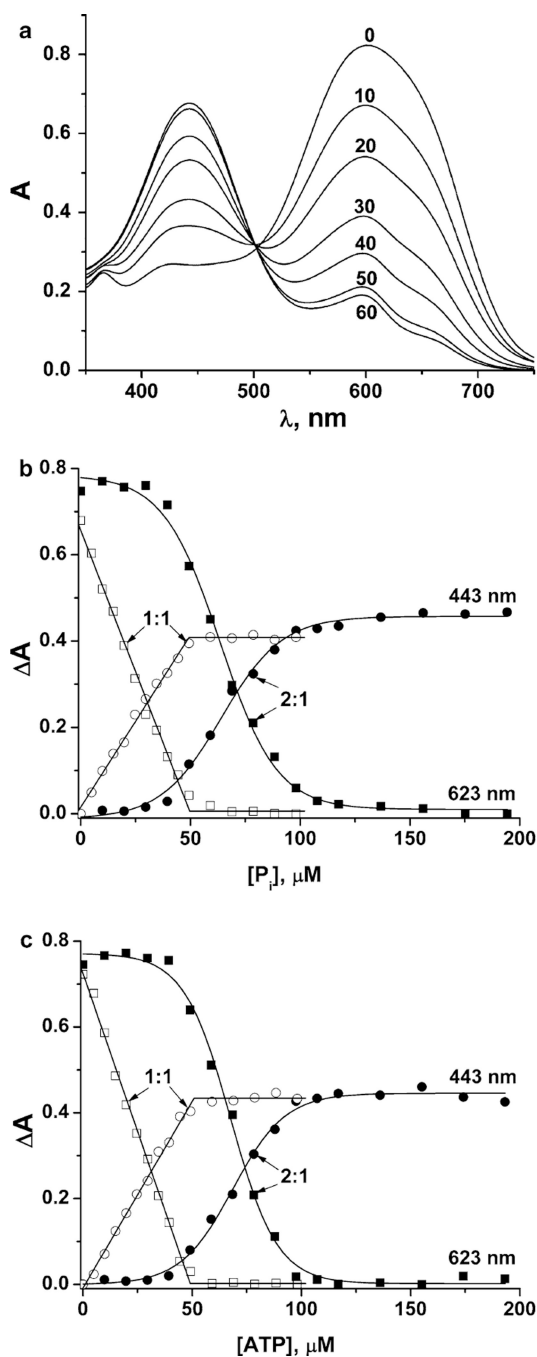


Fig. 4. The absorbance of solutions with a 1:1 Yb^{3+} :PV ratio (50 μM Yb^{3+} and 50 μM PV) in 10 mM HEPES buffer (pH 7.0) (a). The effect of the Yb^{3+} :PV ratio in 10 mM HEPES buffer (pH 7.0) on the absorbance change at 443 nm (*circles*) and 623 nm (*squares*) from phosphate (b), and ATP (c) addition. **Filled symbols** correspond to the absorbance change with a 2:1 Yb^{3+} :PV ratio (100 μM Yb^{3+} and 50 μM PV); *open symbols* to the absorbance change with a 1:1 Yb^{3+} :PV ratio (50 μM Yb^{3+} and 50 μM PV)

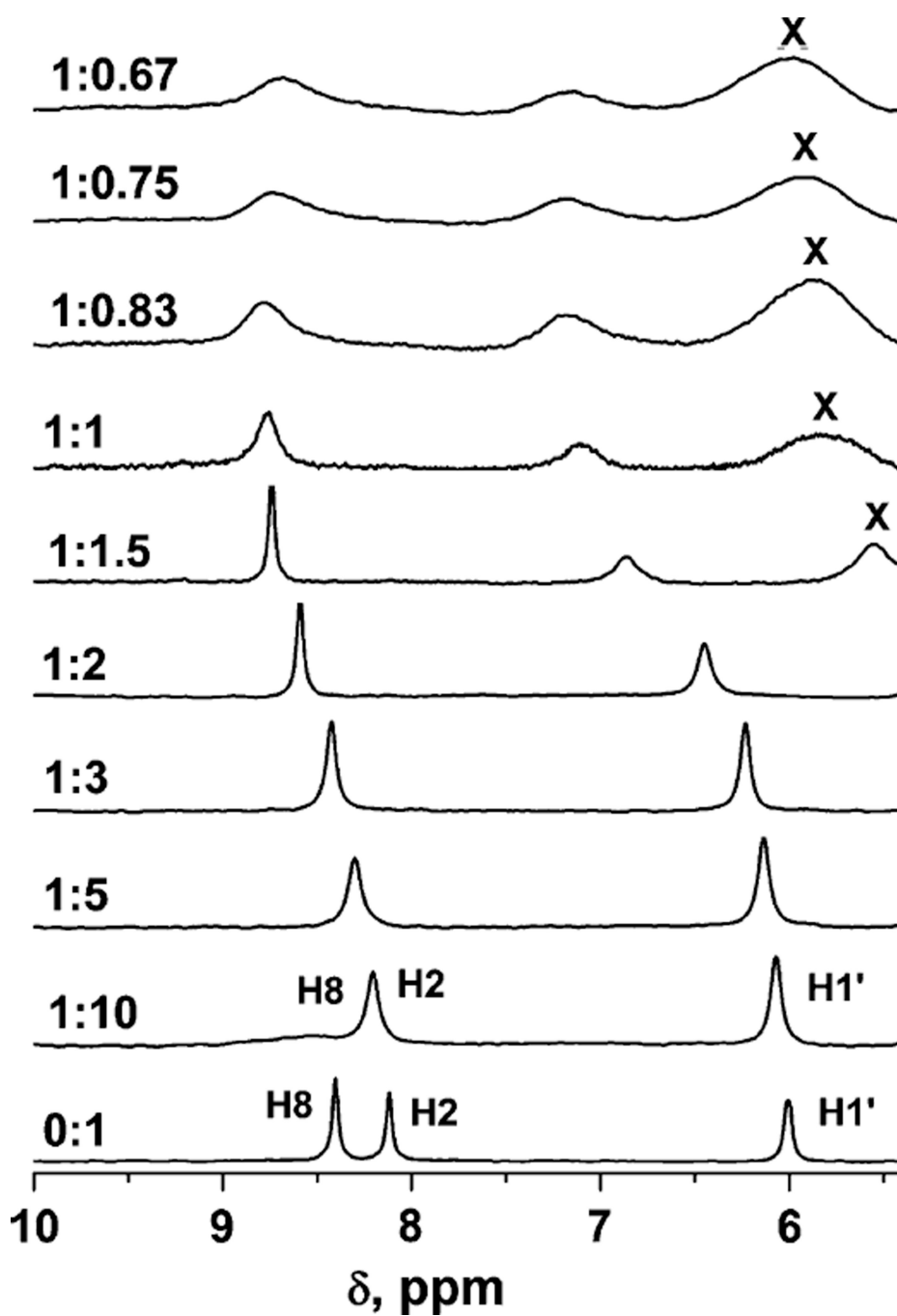


Fig. 5. ^1H NMR spectra of 5 mM ATP solutions with various amounts of added Yb^{3+} . The Yb^{3+} to ATP ratio is shown next to and to the left of the spectra. The solution pH values were between 6.9 and 7.1. Paramagnetic parameters were used to record these spectra (see “Materials and methods”). The ^1H assignments are indicated on the *bottom spectrum*. *X* marks an unassigned proton signal

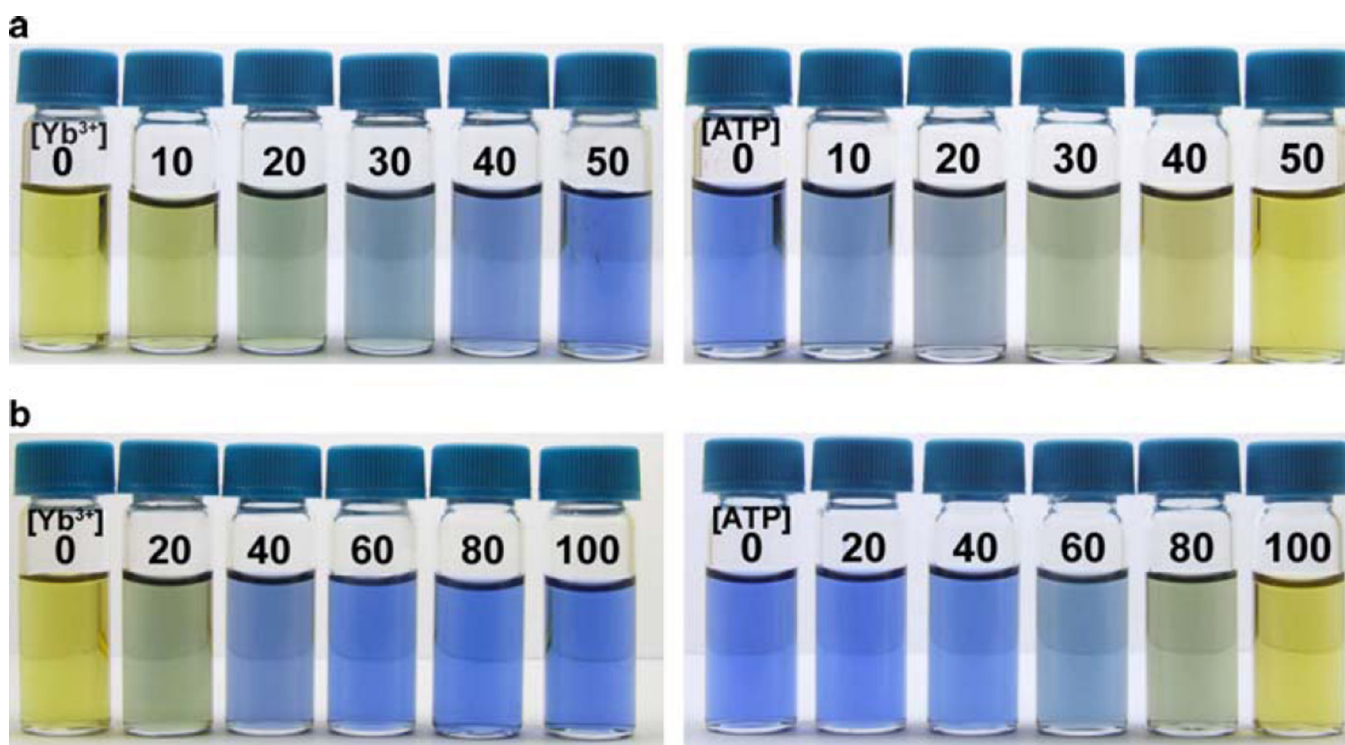


Fig. 6.
a Visual assessment of color changes in PV (50 μM) solutions in HEPES (10 mM, pH 7.0) upon the addition of [Yb³⁺] = 0–50 μM and then [ATP] = 0–50 μM (*top*). **b** Corresponding series for [Yb³⁺] = 0–100 μM and [ATP] = 0–100 μM (*bottom*)